Thermal Contact Conductance of Nominally Flat, Rough Surfaces in a Vacuum Environment

By

M. Michael Yovanovich
Henri Fenech

AIAA Paper No. 66-42 presented at the
3rd Aerospace Sciences Meeting,
New York, NY, January 24-26, 1966.

Progress in Astronautics and Aeronautics, 1966,
Vol. 18, Thermophysics and Temperature Control
of Spacecraft and Entry Vehicles, pp. 773-794.

Thermophysics and Temperature Control of Spacecraft and Entry Vehicles

Edited by

Gerhard B. Heller

NASA George C. Marshall Space Flight Center,
Huntsville, Alabama

A Selection of Technical Papers
based mainly on
the American Institute of Aeronautics and Astronautics
Thermophysics Specialist Conference
held at Monterey, California
September 13-15, 1965

Vol. 18

ACADEMIC PRESS · NEW YORK · LONDON · 1966

THERMAL CONTACT CONDUCTANCE OF NOMINALLY FLAT, ROUGH SURFACES IN A VACUUM ENVIRONMENT

M. Michael Yovanovich* and H. Fenech†

Massachusetts Institute of Technology,
Cambridge, Mass.

Abstract

The steady-state thermal conductance coefficient at the interface formed by nominally flat, rough contacting surfaces placed in a vacuum environment has been investigated for the case of negligible radiation effect. The resistance (reciprocal of conductance) is because of the surfaces of solid bodies, which, when pressed together, actually touch at isolated spots and, therefore, the real contact area is a small fraction of the total or apparent area. Thus the heat transfer across the interface is confined to the contacting spots resulting in converging and diverging heat flow lines at each contact spot. The analysis indicates the conductance is dependent upon the material properties, the surface geometry, and the interface deformation under the applied load. Test results show conclusively that the physical interaction of the surface asperities cannot be treated as purely plastic yielding or purely elastic yielding. The elastic-plastic interaction of the asperities has been taken into consideration by correlating the applied load with a dimensionless parameter which is a function of the surface geometry and the surface deformation due to loading.

Presented as Preprint 66-42 at the AIAA Third Aerospace Sciences Meeting, New York, January 24-26, 1966. The authors gratefully acknowledge the financial support of NASA in sponsoring this work under Research Grant NGR-22-009-065. This work was done in part at the Computation Center at the Massachusetts Institute of Technology, Cambridge, Mass.

*Staff Engineer, Advanced Systems Department, Dynatech Corporation, Cambridge, Mass.

†Associate Professor.

Nomenclature

a = outer radius of heat channel
A_a = total projected apparent area of contact
A_r = total projected real area of contact
c = average radius of contact spot
E = modulus of elasticity; $E_m = 2\,E_1E_2/(E_1 + E_2)$ harmonic mean value
h = thermal conductance coefficient
H = yield pressure (load per unit of projected area)
k = thermal conductivity; $k_m = 2\,k_1k_2/(k_1 + k_2)$ harmonic mean value
N = number of contact spots
n = number of contact spots per unit area
P = applied pressure = W/A
P_a = apparent pressure on contact = W/A_a
Q = heat flow rate per heat channel
R = contact resistance = $\Delta T/Q$
S = surface area
T = temperature
T_o = temperature infinitely far from interface
W = total load on the contact
Y = separation of mean lines
ϵ = $c/a = \sqrt{A_r/A_a}$
σ = root mean square roughness
$\dot{\sigma}$ = root mean square slope
ω = compliance

Subscripts

0 = zero load condition
1,2 = metals 1 and 2, respectively, in contact
a = apparent
e = elastic deformation
m = harmonic mean value
p = plastic deformation
r = real

Introduction

During the past fifteen years many papers and reports on the subject of thermal contact conductance have been stimulated by recent technological developments in the power reactor field and in aerospace work. The very high heat fluxes encountered in reactor design required that the thermal conductance between the fuel elements and the metal cladding should be known to determine the fuel temperature. The aerospace industry on the other hand, required information about the thermal conductance between light-weight materials operating in a vacuum. [1,9,10]

This paper is concerned with the analytical and experimental determination of the steady-state thermal contact conductance between nominally flat (i.e., not wavy) rough surfaces placed in a vacuum environment and operating at an interface temperature such that the radiation is negligible.

Description of Surfaces

A careful examination of profiles of real surfaces obtained by means of surface analyzers, such as the one described by Henry[3] or by any of the several commercial machines available, reveals that real surfaces of solid bodies are both rough and wavy. The roughness component, often referred to as the microscopic roughness, is due to the irregularities on the surface which result from the inherent action of production tools. These are deemed to include traverse feed marks and the irregularities within them. Roughness can range from 2×10^{-6} in. rms for very smooth surfaces to 600×10^{-6} in. rms for the roughest surfaces.

Waviness or macroscopic roughness is that component of the surface profile upon which roughness is superimposed. The waviness may result from such factors as machine or work deflections, vibrations, chatter, heat treatment, or warping strains. The length of these waves, depending on quite a number of conditions, varies from 0.04 to 0.40 in. and the height accordingly varies from 80×10^{-6} to 1600×10^{-6} in. The waviness component can appear as cylinders or spherical caps, and may or may not be periodic in character. A surface without waviness will be called nominally flat in this work. The effect of the surface waviness upon the contact conductance will be considered in a subsequent paper.

The nominally flat, rough surface is characterized by having a series of peaks and valleys. The heights of the asperities seldom exceed 600×10^{-6} in. rms. The most characteristic range of the included angle at the peak is between 160° and 164°. [14,15] The smallest included angle which occurs with the roughest surfaces would seldom be smaller than 150°. The crests or peaks of the asperities are surfaces of very gentle curvature and not as shown in Fig. 1a. The vertical scale is exaggerated with respect to the horizontal scale by a factor of 10 to 100, so that the sides of the peaks and valleys appear much steeper than they really are, and the curvature of the peaks and valleys appears greater than the actual curvature shown in Fig. 1b.

Thermal Analysis

An examination of nominally flat, rough surface profiles shows that, for small compliances (relative displacement of surfaces in the direction of load), as a result of light to moderate pressures, the contact spots are small and few. Each spot is assumed to be circular in area and concentric with the heat channel which supplies the spot. Since the slopes of the asperities which contribute to the contact are generally less than 10^{o}, and the radius of the contact is orders of magnitude smaller than the radius of the heat channel, the system can be regarded as one semi-infinite solid in contact with another over a small circular area. As the applied load is increased, the number and the size of the contact spots increase so that the model proposed for light loads is no longer applicable. In this case, the influence of one contact spot on another must be considered in the analysis.

The thermal conductance of a contact h is defined as the ratio

$$h = (Q/A_a)/\Delta T_c \tag{1}$$

where Q is the heat flow rate through the contact, A_a the total projected area of the contact perpendicular to the direction of heat flow, and ΔT_c the additional temperature drop required to overcome the thermal resistance of the contact. This temperature drop is obtained experimentally by extrapolating the temperature distribution in the heat flow direction from regions outside the disturbance to the contact plane, as shown in Fig. 2.

The thermal contact resistance following the electrical analog is given by

$$R = \Delta T_c/Q \tag{2}$$

and

$$dR = ds/k\,\delta A \tag{3}$$

where k is the thermal conductivity, ds is the elemental length in the direction of the heat flux vector, and dA is the elemental area perpendicular to the heat flux vector.

Combining these definitions one can then write the relationship between the thermal conductance and resistance as

$$\frac{1}{h A_a} = \int dR = \int_s \frac{ds}{\int_A k\,\delta A} \tag{4}$$

The problem of heat transfer with light loading reduces to that of the heat flow between two semi-infinite regions $0 < z_1 < \infty$, $0 < z_2 < \infty$, having thermal conductivities k_1 and k_2 (Fig. 3) which are in contact over the radius c, the center of the contact being taken as the origin of the cylindrical coordinate system (r, θ, z).

The following analysis is based upon steady-state conditions, constant thermal and material properties, clean surfaces (no oxide film resistance), no interstitial fluid (vacuum), and negligible radiation transfer across the voids.

The solution to the differential equation

$$\frac{\partial^2 T}{\partial r^2} + \frac{1}{r}\frac{\partial T}{\partial r} + \frac{\partial^2 T}{\partial z^2} = 0 \qquad (5)$$

for the axially symmetric case (see Appendix A) is

$$T_1 = T_o - \frac{2\,T_o k_2}{\pi(k_1 + k_2)} \int_o^\infty e^{-mz} \sin(mc) J_o(mr) \frac{dm}{m} \qquad (6)$$

$$T_2 = \frac{-2\,T_o k_1}{\pi(k_1 + k_2)} \int_o^\infty e^{-mz} \sin(mc) J_o(mr) \frac{dm}{m} \qquad (7)$$

The contact temperature is therefore

$$T_1 = \frac{T_o k_1}{(k_1 + k_2)} \qquad z = 0 \qquad r < c \qquad (8)$$

and is seen to be independent of the size of the contact and is uniform over the contact area.

The heat flow over the contact area is found by integration to be

$$Q = -2\pi k_1 \int_o^c r \frac{\partial}{\partial z} \left[\frac{2\,T_o k_2}{\pi(k_1 + k_2)} \int_o^\infty e^{-mz} \sin(mc) J_o(mr) \frac{dm}{m} \right]_{z=o} dr \qquad (9)$$

therefore,

$$Q = \frac{4\,k_1 k_2 T_o\, c}{(k_1 + k_2)} = 2\,k_m T_o\, c \qquad (10)$$

It is seen that the heat flow varies linearly with the radius of contact, and the total thermal contact resistance can now be expressed as

$$R = \frac{T_1 - T_2}{Q} = \frac{1}{2 N k_m c} \tag{11}$$

if there are N contact spots over the apparent area A_a.

Combining Eqs. (4) and (11) and defining $c = \epsilon a$, n as the number of contact spots per unit area such that $n\pi a^2 = 1$, and $\epsilon = a/c$, gives an expression for the thermal conductance for light loading

$$h = (2/\sqrt{\pi}) k_m \sqrt{n} \epsilon \tag{12}$$

For the case of high apparent pressure (Fig. 4), where the influence of one heat channel upon another cannot be neglected, the total constriction resistance for N parallel heat channels can be approximately expressed[7,18] as

$$R(N,c) = \frac{2}{2\pi k_m N c} \tan^{-1}\frac{a}{c} - \frac{2a}{k_m N \pi a^2} \tag{13}$$

Since the apparent area $A_a = N\pi a^2$ and $n\pi a^2 = 1$, then by direct substitution the conductance can be written as

$$\frac{k_m \sqrt{n}}{h} = \frac{2}{\sqrt{\pi}} \left[\frac{1}{2\epsilon} \tan^{-1}\frac{1}{\epsilon} - 1 \right] \tag{14}$$

For values of $\epsilon \leq 0.03$, $\tan^{-1} 1/\epsilon$ can be calculated from $[(\pi/2)-\epsilon]$. It can be seen that in the limit as ϵ goes to zero, the right hand side of Eq. (14) reduces to $\sqrt{\pi}/2\epsilon$ and the equation is identical to the equation determined for the case of light to moderate loads.

It is interesting to note that the dimensionless heat transfer number is composed of the contact conductance, the thermal conductivity of the metals, and the square root of the number of contact spots per unit area. The parameter $\sqrt{n}$ is actually the reciprocal of the distance or pitch between contact spots and implicitly takes into consideration the surface geometry and some effects of the applied load.

Surface Deformation

Based upon the thermal analysis of the previous section, it is evident that the two most important surface parameters are the number of contact spots per unit apparent area and the ratio of the real to apparent area. The task of this section is to correlate the surface parameters $\sqrt{n}$ and ϵ with the applied load and the material properties through a dimensionless parameter based on the compliance of the two surfaces.

Determination of $\sqrt{n}$: In order to determine the compliance vs. applied load, we must first obtain values of $\sqrt{n}$ vs. the compliance by considering the interaction of linear profiles of the two contacting surfaces using a profilometer. If we assume that the asperities are randomly distributed over the contacting surfaces, then recorded[11,12] profiles along any diameter of the surface will be representative of any other diameter. This will allow us to obtain the three-dimensional configuration of the surfaces by recording only one profile from each surface. The initial, or no-load position, is determined when contact is first established at three spots. To simulate an increase in pressure, the profiles are moved by small increments in a direction perpendicular to the contact plane; this relative displacement of the two profiles is termed the compliance of the two surfaces under load and will be designated as ω. This technique is best accomplished by reproducing the two profiles on transparent sheets of paper and counting the number of times the surfaces interfere with each other as the compliance is increased. The two profiles are then displaced a slight distance parallel to the contact plane and the counting procedure is repeated as the compliance is increased and the number of contact points is then averaged. The curve of $\sqrt{n}$ vs. the separation of the mean lines is extrapolated to the value $\sqrt{3}$, which is arbitrarily taken as the initial, or no-load position and is designated as Y_o. It is found that the initial separation is three to four times the rms value of the roughness of the surfaces. The graphically determined values of $\sqrt{n}$ vs the dimensionless parameter ω/Y_o for two surface roughness are plotted in Fig. 5. It should be noted that this is a geometric relationship and is therefore independent of the material properties of the surfaces.

Determination of ϵ:[8] The real area of contact between nominally flat, rough surfaces having a random distribution of asperity heights about a mean plane can be approximated by considering the interaction of an ideally-flat, rigid surface with a rough surface having a rms $\sigma = \sqrt{\sigma_1^2 + \sigma_2^2}$, where σ_1 and σ_2 are the rms deviations of surfaces 1 and 2. Assume that all the asperities can be idealized as cones having a distribution of heights and base angles.[16] Since it is known that the base angle (see Fig. 1b) varies only slightly from the rms of the slope, it will be assumed that the tangent of the

base angle is independent of the distance from the mean line. At any penetration y of the rigid flat plane into the rough surface, n asperities per unit area having an average contact radius r are contacted. As the rigid plane moves an incremental distance dy, dn additional asperities are contacted and the following relation

$$A_{(y + dy)} = A_y + dA_y \tag{15}$$

can be written as

$$\pi[n + (dn/dy)dy](r + dr)^2 = n\pi r^2 + dA_y \tag{16}$$

If we assume, based upon continuity of material, that the average contact radius r is linearly proportional to the displacement of the flat surface into the rough surface, we can write

$$dr = dy/\tan\theta \tag{17}$$

Using the result from statistical theory (4) and denoting by j the ratio of the maximum peak to the rms, σ (see Fig. 1a), we have

$$dn/dy = (2nj/\sigma)(1 - y/j\sigma) \tag{18}$$

and neglecting terms of $(dy)^2$ and smaller, it can be shown that

$$dA/A = (2/y)dy + (2j/\sigma)dy - (2y/\sigma^2)\,dy \tag{19}$$

The boundary conditions to be satisfied are at

$$y = 0\ ,\ A_y = 0 \quad \text{and} \quad y = j\sigma\ ,\ A_y = A_a \tag{20}$$

The second boundary condition states that all of the material above the mean plane must flow into the valleys below the mean plane when the compliance has reached its maximum value $j\sigma$.

The solution to Eq. (19) satisfying the boundary conditions yields the following interesting result:

$$\epsilon^2 = (A_y/A_a) = (\omega/Y_o)^2\, e^{-j^2}\,(1 - \omega/Y_o)^2 \tag{21}$$

where ω is the compliance of the two surfaces under an applied load and Y_o is the initial, or no-load, separation of the mean planes. Equation (21) is plotted as a function of the factor j in Fig. 6, where j is a characteristic of the surface if the length of the sample contains many asperities.[22]

If it is assumed that the asperities are deformed plastically, the real contact area can support only the stress at which the material begins to yield. For metallic surfaces, this stress is the microhardness H of the material determined in a Knoop or Vickers test. Since the microhardness for the asperity shape considered is almost 3Y, where Y is the yield stress of the material under tensile forces, the apparent pressure for plastically deformed asperities is given by [13,17,20]

$$P_a = 3Y\,\epsilon^2 \tag{22}$$

If the deformation of the surfaces were assumed to be completely elastic, then the geometric parameter ϵ can be determined from the classical elastic theory of Hertz. The following deformation analysis is based upon these assumptions: 1) all asperities have spherical caps, 2) the number of asperities in contact will be determined by the graphical analysis of profiles, 3) the surfaces are isotropic (i.e., no lay), 4) the two surfaces are of the same material and $\nu_1 = \nu_2 = 0.3$, 5) the two surfaces are similar, i.e., $R_1 = R_2 = R$, 6) the two surfaces are symmetrical about the contact plane, and 7) the line of force always acts through the centers of curvature of contacting asperities.

Elastic theory shows that the following simple geometric relationship between the radius of contact r, the radius of curvature R, and the compliance ω, holds (see Appendix B)[21]

$$r^2 = (\omega R)/2.0 \tag{23}$$

The second geometric parameter can now be determined from

$$\epsilon_e^2 = \frac{A_r}{A_a} = \frac{N_1 \pi r_1^2}{A_a} + \frac{N_2 \pi r_2^2}{A_a} + \frac{N_3 \pi r_3^2}{A_a} + \ldots \tag{24}$$

or

$$\epsilon_e^2 = \frac{\pi}{2.0} \sum_{i=o}^{m} (\omega_m - \omega_i)(n_{i+1} - n_i)\, R_i \tag{25}$$

where the summation over the subscript i is to account for the new contact points which appear when the compliance ω increases by $\Delta\omega$, an arbitrary increment.

Similarly, one can show that the apparent pressure can be related to the surface geometry (n,R), the compliance ω, and the elastic modulus E, by the following relationship:

$$\left(\frac{P_a}{E}\right) = \frac{1}{1.865} \sum_{i=o}^{m} (\omega_m - \omega_i)^{3/2} (n_{i+1} - n_i) R_i^{1/2} \qquad (26)$$

Values of ϵ_e and P_a/E as given by Eqs. (25) and (26) are plotted in Figs. 7 and 8 for different values of j.

To determine whether the asperities deform elastically or plastically we have shown in Fig. 9 the experimental values of h/k_m vs. P_a (apparent pressure). These experiments were performed in our laboratory and are fully described in Ref. 4. In the same figure is shown the calculated values of h/k_m using Eq. (14) where the contact ratio ϵ was obtained using 1) the elastic theory outlined previously and Eq. (25), and 2) the plastic theory using the relationship $\epsilon_p^2 = P_a/H$ where H is the yield pressure, and the corresponding compliance ratio (ω/Y_o) was calculated from Eq. (21). The number of contact points was obtained as in part 1 using Fig. 5 described earlier.

Figure 9 shows that the deformation of the surfaces at light to moderate pressures is due to the plastic deformation of the asperities, but at higher pressures the actual deformation begins to deviate from the completely plastic assumption. At the light pressures the assumption of completely elastic deformation of the asperities is erroneous but at higher pressures this effect seems to be important,and is probably the reason that the experimental observations deviate from the assumption of completely plastic deformation.

The increasing elastic behavior of the contact as the load increases can physically be explained by the following facts. As the load increases the number of contact spots also increases. This produces an increasing but more uniformly distributed pressure on the apparent area of contact. Most of the contact spots have already been plastically deformed at the utmost and further deformation has to take place by elastic displacement of the sublayers.

Since the phenomenon of surface interactions at large pressures is quite complex and therefore intractable, it was decided to obtain empirical information about the surface interactions under loading conditions. A survey of the literature revealed that several

authors had investigated this mechanical phenomenon under various surface conditions, geometries, and physical loads. Invariably the investigators were concerned with relatively smooth surfaces under very light loading so that only a small number of asperities per unit area were contacted, and therefore the deformation of these contacted asperities was completely plastic.

The most interesting and useful paper[19] showed experimental data of applied load vs. surface separation for three metals. In the present work, the aluminum and stainless steel data have been replotted as the apparent pressure vs. the dimensionless compliance, Figs. 10 and 11. Since empirical data of the apparent pressure against the dimensionless compliance for these metals at higher pressures were not available, it was decided to use experimental information, such as $\sqrt{n}$ vs P_a for aluminum surfaces (Fig. 12) and h/k_m vs P_a for the stainless-steel surfaces (Fig. 9).

With the assumption that $\sqrt{n}$ vs compliance is a geometric relationship independent of the material under consideration, then the apparent pressure as a function of the dimensionless compliance for any metal can be obtained from empirical data relating the number of contact spots per unit area against the apparent pressure. The information in Fig. 12 is shown cross plotted in Fig. 10 and compares quite favorably with the information in Ref. 19. The heat-transfer data for stainless-steel surfaces yielded the plot of Fig. 11, which shows again a very satisfactory correlation of data from two independent sources.

The experimental data[19] was obtained for metals which had relatively smooth surfaces, and for light apparent pressures that never exceeded 120 psi; whereas the other experimental data was obtained for surfaces that were, relatively speaking, much rougher and the pressures ranged from a minimum of 130 psi to a maximum of about 15,000 psi.

The good agreement under these conditions is therefore most encouraging and suggests that the basic assumptions are quite good. An examination of Figs. 10 and 11 shows that, when the apparent pressure is plotted against the dimensionless compliance, the effect of the surface roughness is not very strong. However, further load-compliance tests should be made for various materials having a range of roughnesses before definite conclusions can be made.

To check out the basic assumptions and the conclusions drawn from the load-compliance plots, test data for stainless steel surfaces, one of which was very smooth, whereas the other had a roughness of 42×10^{-6} in., were compared with the predicted values based upon Figs. 5, 6, 11 and the thermal conductance equation (14), Fig. 13. Extremely good agreement was obtained between theory and test over the entire load range.

Conclusions

The thermal contact conductance equation is in good agreement with the experimental results when the geometric parameters are determined from experimental load-compliance data. The graphical method proposed for determining the geometric parameter $\sqrt{n}$ and Eq. (21) determined from geometric and continuity considerations gave good results for the two cases. This method is therefore considered to be applicable for any contact between nominally flat, rough surfaces in a vacuum environment. Since the actual deformation of the surface or surfaces appears to be plastic at light loads and then elastic-plastic at higher loads, no one theory, at the present, is capable of predicting the actual number of contact spots and the real area of contact under all surface geometries and apparent pressures. One therefore must resort to experimental data to obtain these geometric parameters.

Appendix A

The solution of Eq. (5) must satisfy the following boundary conditions throughout the two regions:

$$\partial T_1/\partial z = -\partial T_2/\partial z = 0 \quad z = 0 \quad r > c \tag{A1}$$

which states that there is no heat flow across the voids. In the absence of sources or sinks the conservation of energy requires that

$$k_1(\partial T_1/\partial_z) = -k_2(\partial T_2/\partial z) \qquad z >> 0 \tag{A2}$$

and temperature continuity across the contact requires that

$$T_1 = T_2 \qquad z = 0 \qquad r < c \tag{A3}$$

Letting

$$T_1 = T_o \quad \text{at} \quad z_1 = \infty \tag{A4}$$

and

$$T_2 = 0 \quad \text{at} \quad z_2 = \infty \tag{A5}$$

it can be shown by direct substitution that[5]

$$T_1 = T_o - \int_o^\infty \psi(m)\, e^{-mz}\, J_o(mr)\, dm \qquad (A6)$$

and

$$T_2 = \int_o^\infty \phi(m)\, e^{-mz}\, J_o(mr)\, dm \qquad (A7)$$

for any m.

Satisfying the boundary conditions specified previously, the unknowns $\psi(m)$ and $\phi(m)$ can be determined to be[6]

$$\phi(m) = \frac{k_1}{k_2}\,\psi(m) \quad \text{and} \quad \psi(m) = \frac{2\,T_o k_2 \sin(mc)}{m\pi\,(k_1 + k_2)} \qquad (A8)$$

Appendix B

From classical elastic theory the radius of contact r and the compliance ω for two balls in contact are given by

$$r = \left[\frac{3\pi}{4}\, \frac{F(k_1 + k_2)R_1R_2}{(R_1 + R_2)} \right]^{1/3} \qquad (B1)$$

$$\omega = \left[\frac{9\pi}{16}^2\, \frac{F^2(k_1 + k_2)^2(R_1 + R_2)}{R_1R_2} \right]^{1/3} \qquad (B2)$$

Assuming that both spheres have the same elastic properties and taking $\nu = 0.3$, this becomes

$$r = 1.109 \left[\frac{F}{E}\, \frac{R_1R_2}{(R_1 + R_2)} \right]^{1/3} \qquad (B3)$$

$$\omega = 1.23 \left[\frac{F^2}{E^2}\, \frac{(R_1 + R_2)}{R_1R_2} \right]^{1/3} \qquad (B4)$$

References

[1] Fenech, H., "The thermal conductance of metallic surfaces in contact," Massachusetts Institute of Technology, Sc.D. Thesis (May 1959).

[2] Foster, E.T., "Prediction of contact population in bimetallic surface junctions," Massachusetts Institute of Technology, M.S. Thesis (August 1964).

[3] Henry, J.J., "Thermal contact resistance," Massachusetts Institute of Technology, Sc.D. Thesis (August 1964).

[4] Yovanovich, M.M., "Thermal contact conductance in a vacuum," Mechanical Engineering Thesis, Massachusetts Institute of Technology (February 1966).

[5] Carslaw, H.S. and Jaeger, J.C., Conduction of Heat in Solids (Oxford University Press, London, 1959), 2nd Edition.

[6] Watson, G.N., Bessel Functions (Cambridge University Press, Cambridge, 1945).

[7] Cetinkale, T.N. and Fishenden, M., "Thermal conductance of metal surfaces in contact," International Conference on Heat Transfer (1951).

[8] Henry, J.J. and Fenech, H., "The use of analog computers for determining surface parameters required for prediction of thermal contact conductance," J. Heat Transfer (September, 1964).

[9] Shlykov, Yu. P., Gamin, E.A., and Demkin, N.B., "Analysis of contact heat exchange," Redstone Scientific Information Center Report RSIC-177 (1960).

[10] Boeschoten, F. and Van der Held, E.F.M., "The thermal conductance of contact between aluminum and other metals," Physica, XXIII (1957).

[11] Archard, J.F., "Contact and rubbing of flat surfaces," J. Appl. Phys. 24, 8 (August 1953).

[12] Archard, J.F., "Single contacts and multiple encounters," J. Appl. Phys. 32, 8 (August 1961).

[13] Bowden, F.P. and Tabor, D., Friction and Lubrication (Metheun and Co., Ltd., London, and John Wiley and Sons, Inc., New York, 1956).

[14] Dorinson, A., "Microtopography of finely ground steel surfaces in relation to contact and wear," Am. Soc. Lubrication Engrs. Trans. 8 (1965).

[15] Furey, M.J., "Surface roughness effects on metallic contacts and friction," Am. Soc. Lubrication Engrs. 6 (1963).

[16] Greenwood, J.A. and Williamson, J.B.P., "The contact of nominally flat surfaces," Burndy Research Div., Res. Rep. 15 (July 1964).

17 Hoffman, O. and Sachs, G., Introduction to the Theory of Plasticity for Engineers (McGraw-Hill Book Co., Inc., New York, 1953).

18 Holm, R., Electric Contacts Handbook (Springer-Verlag, Berlin/Gottingen/Heidelberg, 1958).

19 Ling, F.F., "On asperity distributions of metallic surfaces," J. Appl. Phys. 29, 8 (August 1958).

20 Nadai, A., Theory of Flow and Fracture of Solids (McGraw-Hill Book Co., Inc., New York, 1950), Vol. I.

21 Timoshenko, S. and Goodier, J.N., Theory of Elasticity (McGraw-Hill Book Co., Inc., New York, 1951).

22 Tarasov, L.P., "Relation of surface-roughness readings to actual surface profiles," Trans. Am. Soc. Mech. Engrs. 67, 189 (1945).

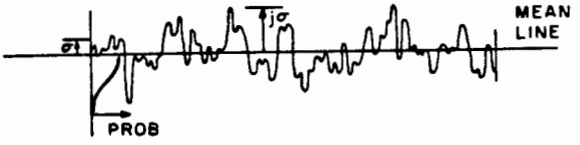

Fig. 1a Typical surface profile.

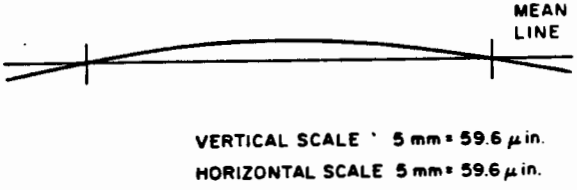

Fig. 1b Typical asperity.

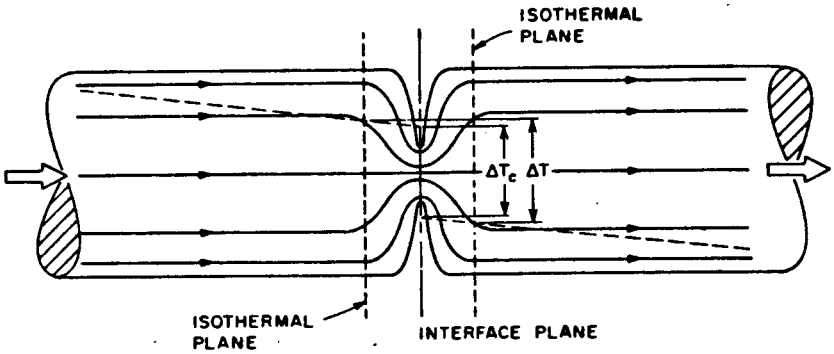

Fig. 2 Typical cylindrical heat channel.

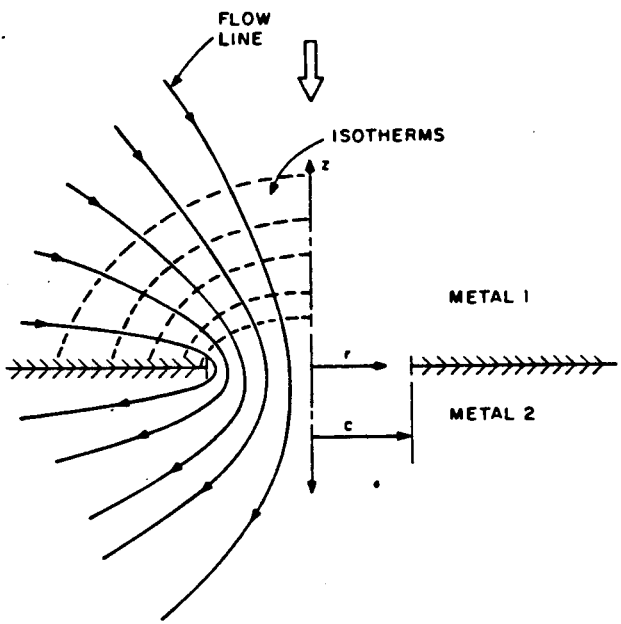

Fig. 3 Contact model for light apparent pressure.

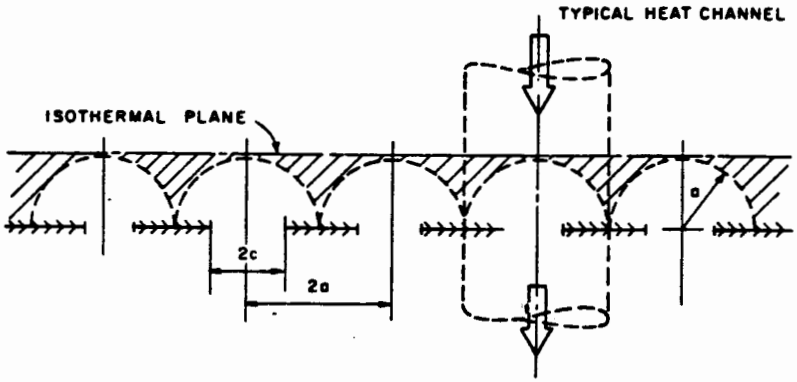

Fig. 4 Contact model for multiple contacts.

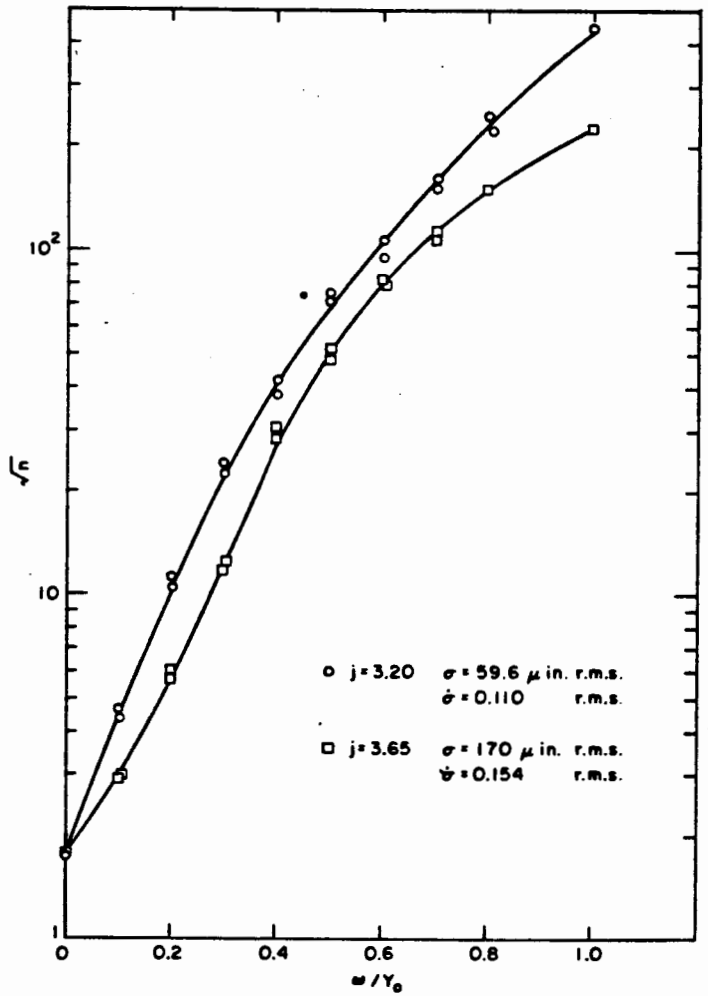

Fig. 5 Contact points vs compliance ratio.

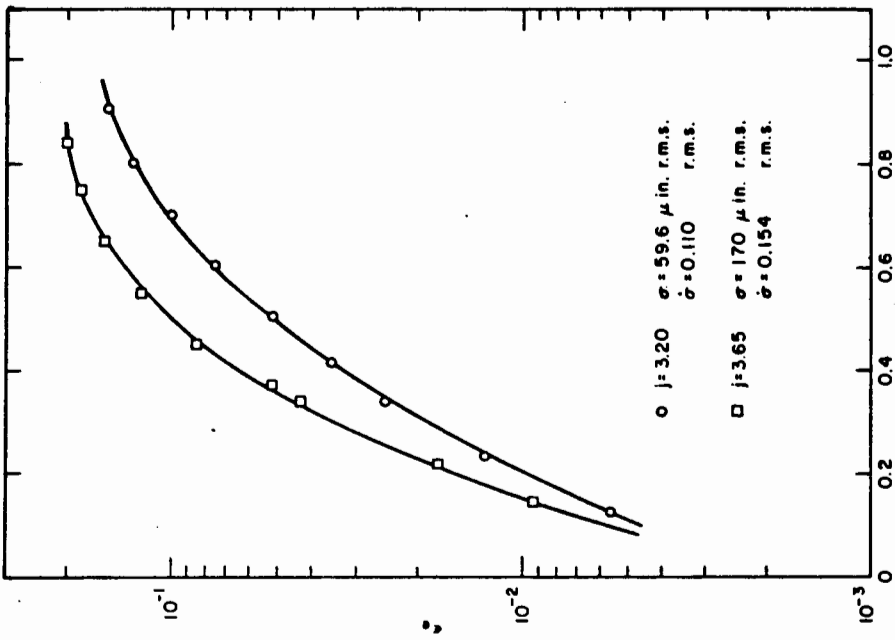

Fig. 7 Area ratio vs compliance ratio.

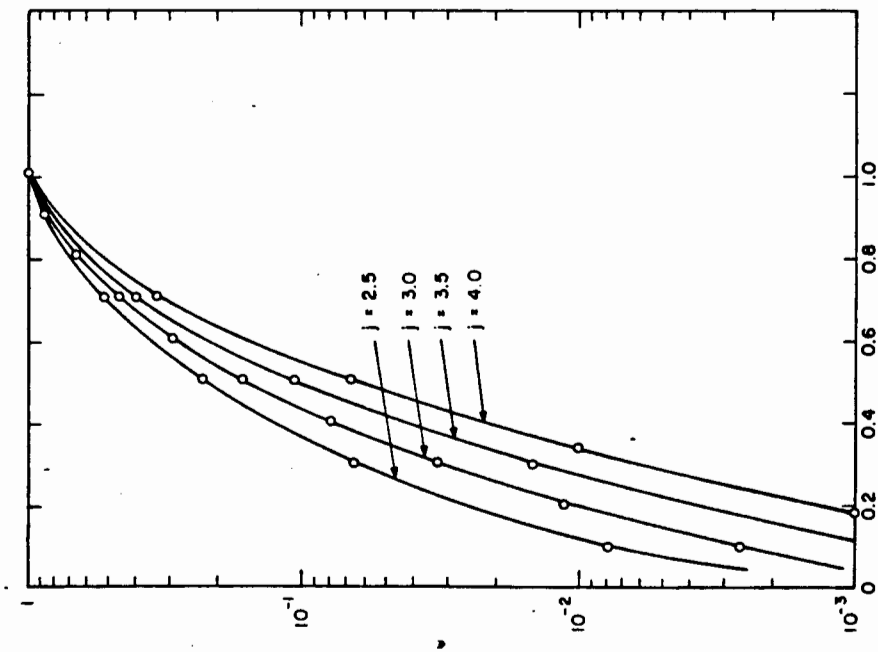

Fig. 6 Area ratio vs compliance ratio.

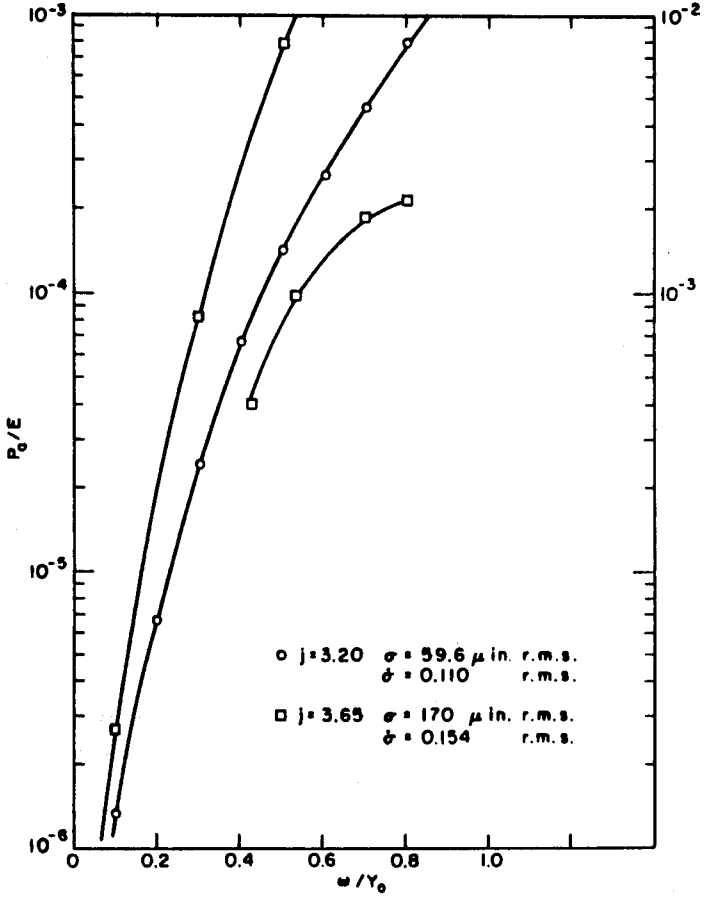

Fig. 8 Apparent pressure vs compliance ratio.

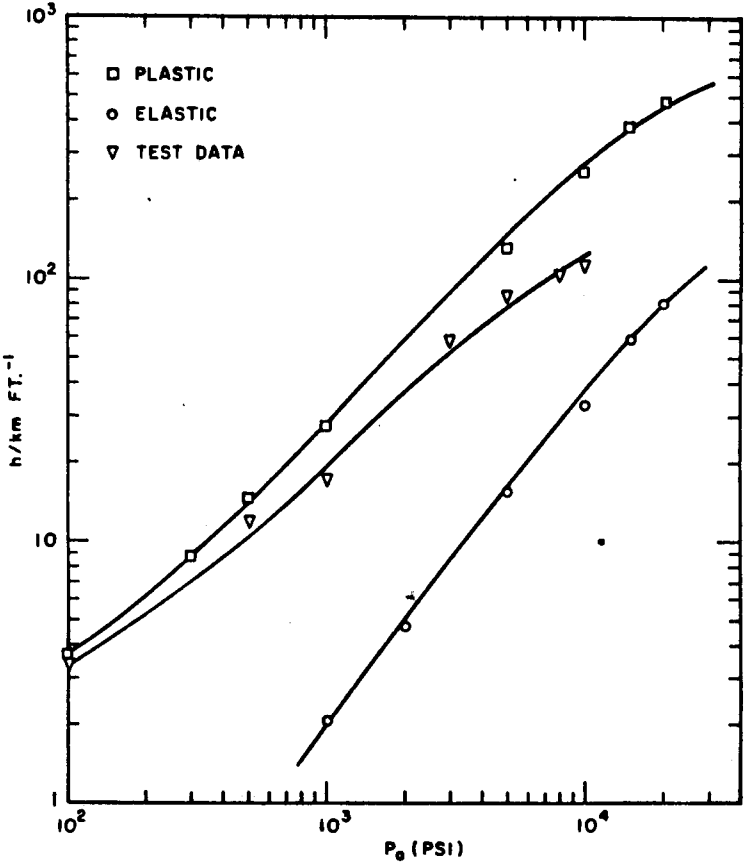

Fig. 9 Heat transfer coefficient vs apparent pressure.

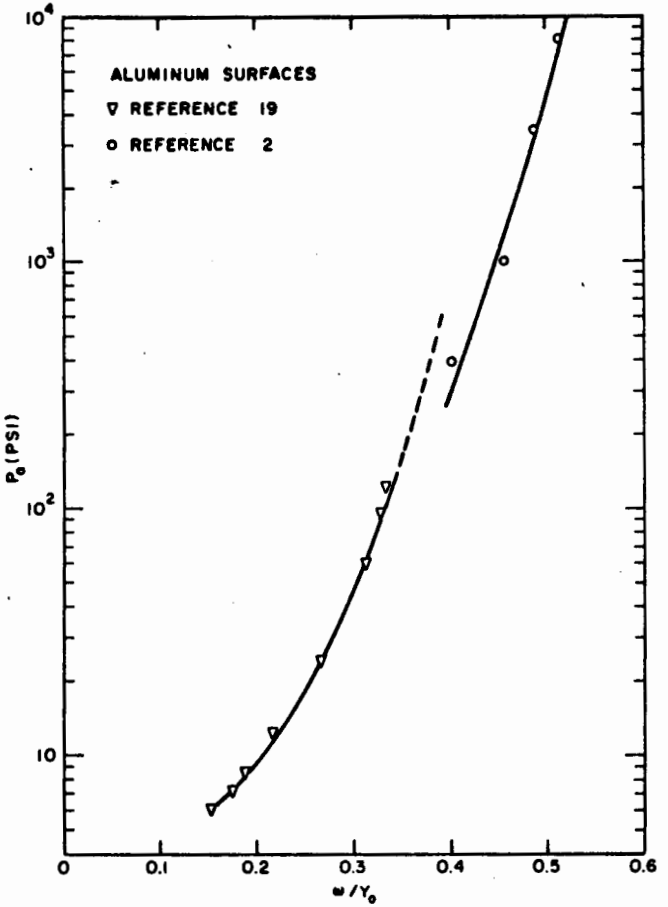

Fig. 10 Apparent pressure vs compliance ratio.

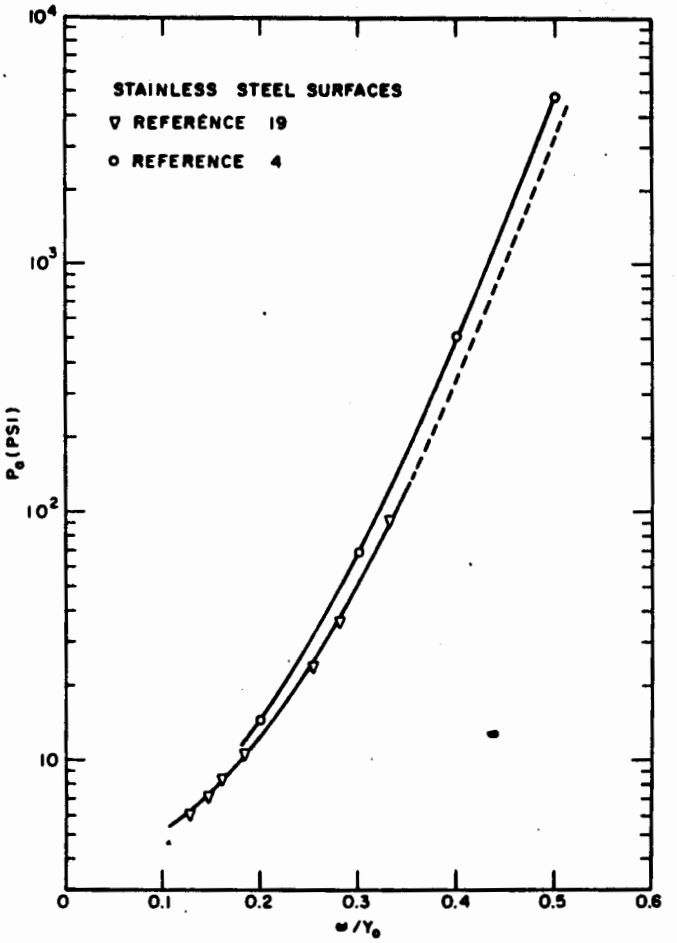

Fig. 11 Apparent pressure vs compliance ratio.

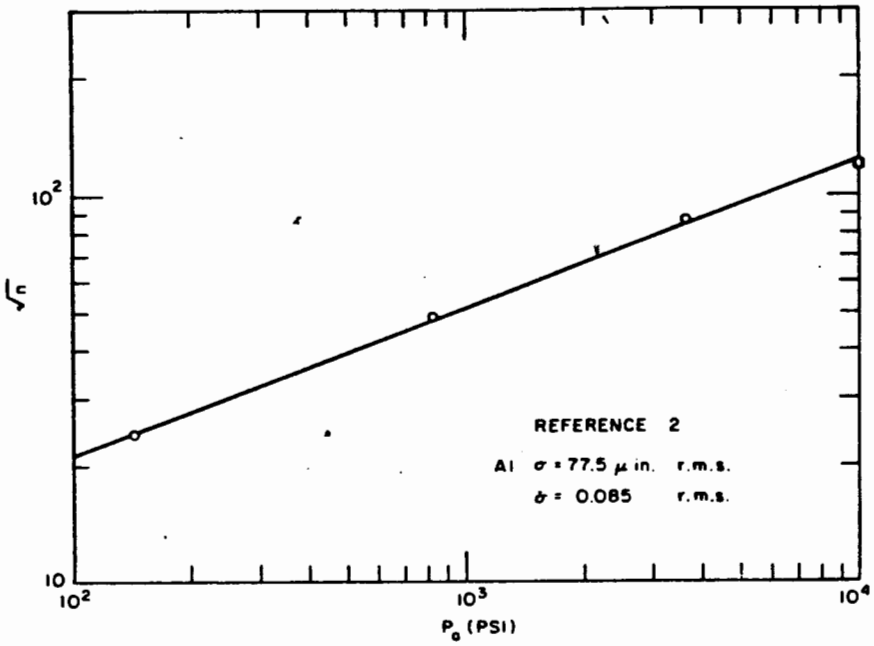

Fig. 12 Contact points vs apparent pressure.

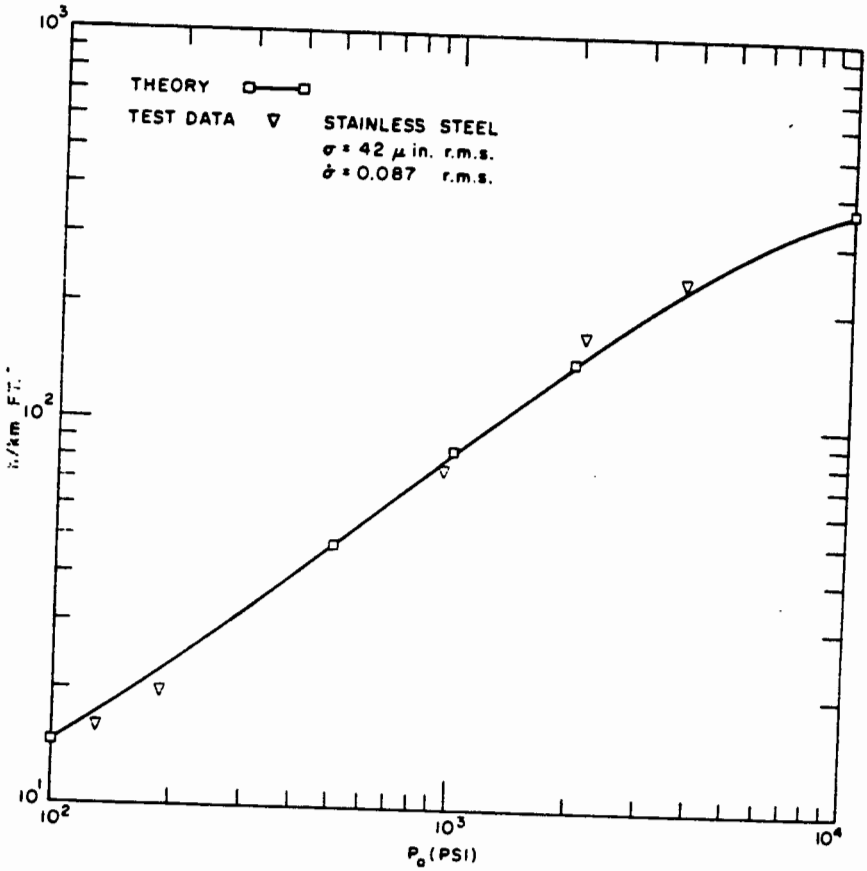

Fig. 13 Heat transfer coefficient vs apparent pressure.